Research articles

Ab initio study of the magnetic, optical and electronic properties of spinel Co_3O_4 within DFT and GW approaches

Vyacheslav S. Zhandun[a,b,*], Andrey Nemtsev[a]

[a] *Kirensky Institute of Physics - Federal Research Center "Krasnoyarsk Science Centre, Siberian Branch of the Russian Academy of Sciences", 660036 Krasnoyarsk, Russia*
[b] *Reshetnev Siberian State University of Science and Technology, 660037 Krasnoyarsk, Russia*

ABSTRACT

The spinel cobalt oxide Co_3O_4 is an antiferromagnetic semiconductor containing two non-equivalent Co^{2+} and Co^{3+} cobalt ions with different local environments and different magnetic moments. We have performed ab initio study and comparison of the electronic, magnetic and optical properties of Co_3O_4 within GGA, GGA + U, and G0W0 approximations. GGA correctly predicts Co_3O_4 to be a semiconductor, but severely underestimates the bandgap. G0W0 approximations increase the bandgap indicating a better description of the cobalt localized d-states. The spectral weights of the bands near Fermi energy are about 0.5. Ab initio calculations confirm that the low-spin state of Co^{3+} ion arises due to the local environment and the crystal effect field. The investigation of the pressure dependencies of magnetic properties revealed the appearance of Co^{3+} ion abrupt transition from low-spin state to high-spin state under tensile pressure. This allows manipulating the spin state of Co^{3+} ions through the pressure or strain.

1. Introduction

The compounds with spinel structure attract great attention as fundamental as well as applied due to their potential applications in various fields of microelectronic such as memory drives, solid fuel cells, lithium-ion batteries, microwave, and radio frequency devices [1–6]. The crystal structure of normal spinel has general configuration AB_2O_4, where A- and B- sites are occupied by bivalent and trivalent cations correspondingly. In the dependence on the cations on the A- and B- sites spinels can show various magnetic, optical and electronic properties. For example, Fe_3O_4 and its alloys demonstrate unusual physical properties [7,8], including large magnetic moment, magnetoresistance, half-metallic behavior.

One more possibility is the application of spinels as the material for spintronics. Nowadays, the spintronic has attracted increasing interest due to its promising applications in the storage and recording devices [9–11], different sensors [12], and logic devices [13]. Recently, it was reported about progress in the room temperature metal-induced crystallization of spinel $CoFe_2O_4$ thin films [14]. The manipulation of the spin degrees of freedom and magnetic properties in materials is crucial for the needs of spintronics [15,16]. Still, researchers have attempted to control the magnetic properties of solid-state materials by various methods, such as light irradiation [17], electric and magnetic fields [18–21], temperature [22], and strain [23].

In the present paper, we perform the results of ab initio investigation of the magnetic, electronic and optical properties of the spinel cobalt oxide (Co_3O_4) including the pressure dependencies of the magnetic and optical properties. The Co_3O_4 is a magnetic semiconductor that has wide applications in energy and environment-related areas [24–29]. Despite so many promising applications of the Co_3O_4 compound, its magnetic properties are not well exploited, partly due to its complex magnetic structures. It is known that Co_3O_4 contains both Co^{2+} in the tetrahedral sites and Co^{3+} ions in the octahedral sites of face-centered cubic (FCC) lattice of oxygen anions. Co_3O_4 undergoes a magnetic transition from paramagnetic to antiferromagnetic state at Neel temperature below 40 K [30–32]. As reported in Ref. [30], the magnetic moment of Co^{2+} in the antiferromagnetic state is equal to $3,26\mu_B$ at 4,2K. The results reported in the literature, based on optical measurements mainly, usually described a bandgap of $\approx$ 0.8–1.6 eV [33–35]. It is necessary also to note the possibility of the presence of a magnetoelectric effect in the spinel family. Nowadays, only a few compounds in the spinel family, e.g., $CoCr_2O_4$ [36] and $ZnCr_2Se_4$ [37], are known to exhibit magnetoelectric properties [38]. However, recently, the experimental observation of the polarization in Co_3O_4 was reported in Refs. [39,40].

First-principles theoretical studies of the properties of bulk Co_3O_4 are not so numerous [41–44] and some issues are yet not under consideration. For example, although several ab initio calculations of the

---

electronic and magnetic properties of Co_3O_4 were performed early, the calculations of optical properties, including their dependence on pressure, are practically absent in the literature. Moreover, all ab initio calculations were performed within different modifications of density functional theory (DFT). However, as known, these methods are designed and applied for the calculation of the ground-state properties only [45]. This raises some doubts that the band structure obtained within the framework of DFT or DFT with gradient corrections (DFT-GGA) can be interpreted as energies of excited states.

For this reason, it is interesting to compare the results of calculations within the DFT-GGA approach and, so-called, GW approximation (where G is electron Green's function and W is screened Coulomb potential). And, at last, as it was mentioned above for the spintronics applications it is critical to have a possibility to manipulate the spin degrees of freedom. To check this possibility in the case of the Co_3O_4 spinel we study the effect of pressure on the magnetic moments of both Co^{2+} and Co^{3+} ions. Thus, the main objective of the present work is to provide a complex theoretical analysis of the structural, electronic, magnetic and optical properties of Co_3O_4 including their dependence on the tensile and compressive pressure in the framework of ab initio approach within different approximations.

The paper is organized as follows. In Sec. II we give a short description of the computational details, in Sec. IIA the comparison of magnetic, optic and electronic properties obtained within three approximations (GGA, GGA + U, and G0W0) are given and in Sec. IIB we present the calculations of pressure dependencies of magnetic and optical properties of Co_3O_4. In the last Section, we make conclusions.

2. Calculation details

All ab initio calculations presented in this paper are performed using the Vienna ab initio simulation package (VASP) [46] with projector augmented wave (PAW) pseudopotentials [47]. The valence electron configurations $3d^7 4s^2$ are taken for Co atoms and $3s^2 3p^4$ for O atoms. The calculations are based on the density functional theory where the exchange-correlation functional is chosen within the Perdew-Burke-Ernzerhoff (PBE) parameterization [48] and the generalized gradient approximation (GGA) has been used. Throughout all calculations, the plane-wave cutoff energy 500 eV is used. The Brillouin-zone integration is performed on the $8 \times 8 \times 8$ Monkhorst-Pack mesh of special points [49]. GGA + U calculations were performed within Dudarev's approximations [50] with U = 4.5 eV for Co ion (following Ref. [51]). In the GW part of calculations implemented in VASP [52], we report the results obtained within the most commonly used G0W0 approximation. In this approximation, the output of DFT-GGA calculations is used as an input for G0W0 calculations and only one iteration is made, i.e., the expansion of the electron Green's function is performed for the exchange-correlation potential in the DFT-GGA approach. We use a small complex shift $\eta = 0.047$ for Kramers-Kronig transformation of dielectric permeability, providing more accurate results. In the present calculation, the chosen number of frequencies was 500 for G0W0 calculations.

3. Results and discussion

3.1. A. Magnetic, optical and electronic properties within GGA, GGA + U, and G0W0 approximations

At room temperature, the cobalt oxide Co_3O_4 (Fig. 1) has a normal spinel structure with an fcc unit cell (space symmetry group $Fd\bar{3}m$). In all calculations, we have used the rhombohedral unit cell containing six cobalt ions and eight oxygen ions. The unit cell contains two non-equivalent cobalt ions with different valence, namely, two Co^{2+} ions and four Co^{3+} ions which are locating on tetrahedral and octahedral sites, correspondingly. Four oxygen ions forming a tetrahedron
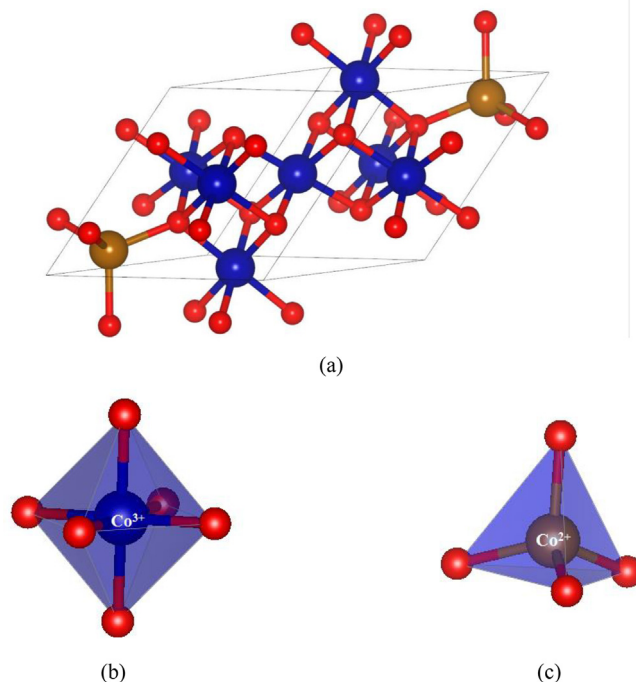

Fig. 1. Unit cell of Co_3O_4 (a), CoO_6 octahedron (b) и CoO_4 tetrahedron (c). Brown, blue and red balls show Co^{2+}, Co^{3+} and oxygen ions, correspondingly. (For interpretation of the references to colour in this figure legend, the reader is referred to the web version of this article.)

surrounds bivalent cations, and trivalent ions are surrounded by six oxygens ions located in the vertices of the octahedron. At that, each oxygen ions is connected with one bivalent and three trivalent cobalt ions. The geometry of the structure was fully optimized within GGA. The calculated optimized lattice parameter of Co_3O_4 a = 8.09 Å is very close to experimental ones [30,53]. The G0W0 calculations have been performed with the same structural parameters.

As an initial step, we calculated the energy of the ground magnetic state of Co_3O_4. As can be seen from Table 1 the antiferromagnetic state is more energy favorable than the ferromagnetic one. In this state, the magnetic moments on Co^{2+} ions located in the center of oxygen tetrahedra are antiparallel and have the absolute value μ = 2,26 μB, whereas magnetic moments on four Co^{3+} ions are equal zero. We also calculated the different magnetic structures with non-collinear directions of magnetic moments on Co^{2+} ions by taking into account spin–orbit coupling (SOC). As can be seen from Table 2, the antiferromagnetic state with the ordering of magnetic moments along [1 1 1] direction is the most favorable by energy. It should be noticed that the experimental investigation of the magnetic structure in Ref. [40] also reveals that magnetic moments are ordering along [1 1 1] direction. The calculated energies of spin–orbit coupling (SOC) for Co^{2+} and Co^{3+} ions are differ: $E_{SOC}(Co^{2+}) = -0.019$ eV and $E_{SOC}(Co^{3+}) = -0.027$ eV.

As an oxide semiconductor with a transition metal having a complex magnetic structure, Co_3O_4 is rather difficult to describe using ab-initio methods. The underestimating of the bandgap of transition metal compounds are known to lack of density functional theory (DFT)

Table 1
The total energies (E) and magnetic moments (μ) on Co^{2+} ions for ferromagnetic (F) and antiferromagnetic (AF) ordering of magnetic moments.

Magnetic ordering	E (eV)	μ (μB)
F	− 94,582	2,21
AF	− 96,088	± 2,26

Table 2
The total energies (E) of Co_3O_4 for different directions of magnetic moments on Co^{2+} ions.

Direction of magnetic moments on both Co^{2+} ions	E (eV)
[1 1 1]	
[1 1 0]	−96,145
[1 1 0]	
[-1-1 0]	−96,162
[1 1 1]	
[-1-1-1]	−96,163
[1 1 1]	
[-1 1 1]	−96,138
[1 0 0]	
[0 1 0]	−96,158
[1 0 0]	
[1 1 1]	−96,161

Fig. 2. Total densities of electronic states (DOS) near the Fermi energy for Co_3O_4 in GGA (black line), GGA + U (red line) and G0W0 (blue line) approximations. The zero on the energy axis is the Fermi energy. Negative values of DOS correspond to the spin-down states. (For interpretation of the references to colour in this figure legend, the reader is referred to the web version of this article.)

(a)

(b)

Fig. 3. Band structure of Co_3O_4 obtained within (a) GGA (black line), (b) GGA + U (red line) and G0W0 (blue points) approximations. Bottom panel shows band structure near the Fermi level. The zero on the energy axis is the Fermi energy. (For interpretation of the references to colour in this figure legend, the reader is referred to the web version of this article.)

approach. To overcome this problem Hubbard repulsion U is often taking into account within the DFT + U scheme. However, this approach also is not without lack, namely, the choice of U and the problem of double accounting. Although there are many different forms of double-counting corrections that are in use [54], it is rather difficult to make a convincing derivation of the right form of this correction due to the non-linear nature of the DFT approach. In turn, the GW method has proved its worth in the description of compounds with transition metals. Moreover, the GW method allows describing excited states more correctly than the DFT approach, which is especially important when describing the energy gap in semiconductors. Therefore we perform the calculation of Co_3O_4 electronic properties using a GGA + U approach as well as G0W0 approximation in conjunction with standard DFT-GGA. The obtained DOS is shown in Fig. 2. The states in the range of [−2.5, +2] eV around Fermi energy are formed by d-states of both Co ions with a slight admixture of p electrons of O and Co. The valent p electrons of oxygen ions are delocalized in the wide energy region of [−8.5, −3.5] eV along with a slight admixture of Co d-electrons. As seen we obtain the presence of the energy gap within the DFT-GGA approach but its width is quite small (about 0.2 eV) as compared with experimental data. GGA + U and G0W0 approximations result in a slight increase in the bandgap. G0W0 approximation makes the bandgap about 0.6 eV while GGA + U make it about 0.35 eV. At that G0W0 shifts deeper valence bands stronger than bands near the Fermi energy.
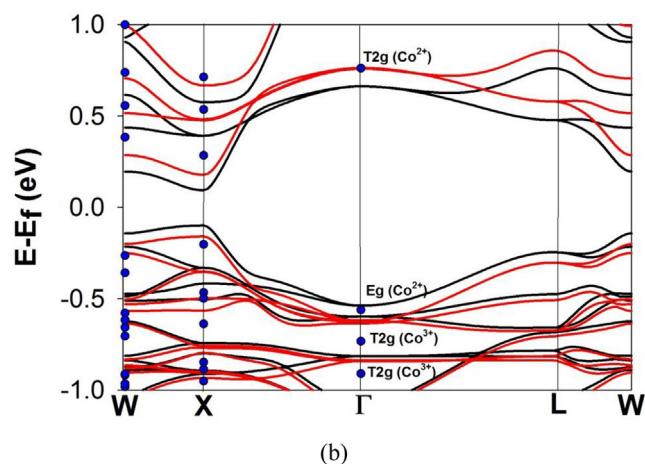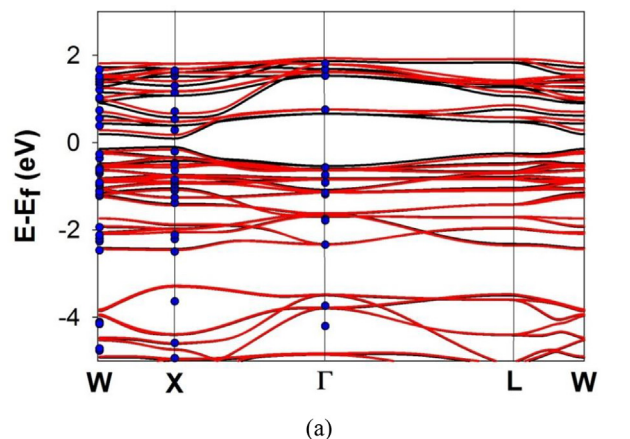
The band structures obtained within three approximations are shown in Fig. 3. The classifications of bands are given following their symmetries in the point Γ of Brillouin zone. The most bands near the Fermi energy are formed by d-states of both Co ions with a small admixture of p-states of O atoms for conductive bands. The eg-electrons of Co^{2+} atoms form the closest to the Fermi energy filled band (Eg), whereas the t2g-states of Co^{2+} atoms form the first empty band (T2g). In the greater part of the Brillouin zone, the gap width is about 1 eV (the maximal value is in Γ point), however in W-X and Γ-W directions the gap narrows. The maxima of the valence band and the minima of conductivity band are located in the X point of Brillouin zone, where the bandgap narrows down to 0.2 eV within GGA approximation. GGA + U and G0W0 approximations result in the shift of bands away from the Fermi level. At that G0W0 approximation shift the bands stronger than GGA one (on the average by 0.15–0.2 eV).

One more strong advantage of the GW approach is the possibility of the description of the spectral weights of quasiparticle states. The spectral weights (as they defined in Ref [52]) can be viewed as an indicator of the interaction strength in k space. Indeed, in a system with no interaction or with weak interaction between electrons spectral weight Z_{nk} is close to unity, whereas in the systems with the interaction between electrons $Z_{nk} < 1$ and it decreases when the interaction becomes stronger. Therefore the analysis of spectral weights behavior provides a deeper understanding of the electronic properties of a material. We obtain that the spectral weight Z_{nk} for bands near the Fermi energy much less than unity, and it ranges from $Z_{nk} = 0.45$–0.47 for valence bands to $Z_{nk} = 0.51$–0.54 for conductive bands. Thus, the
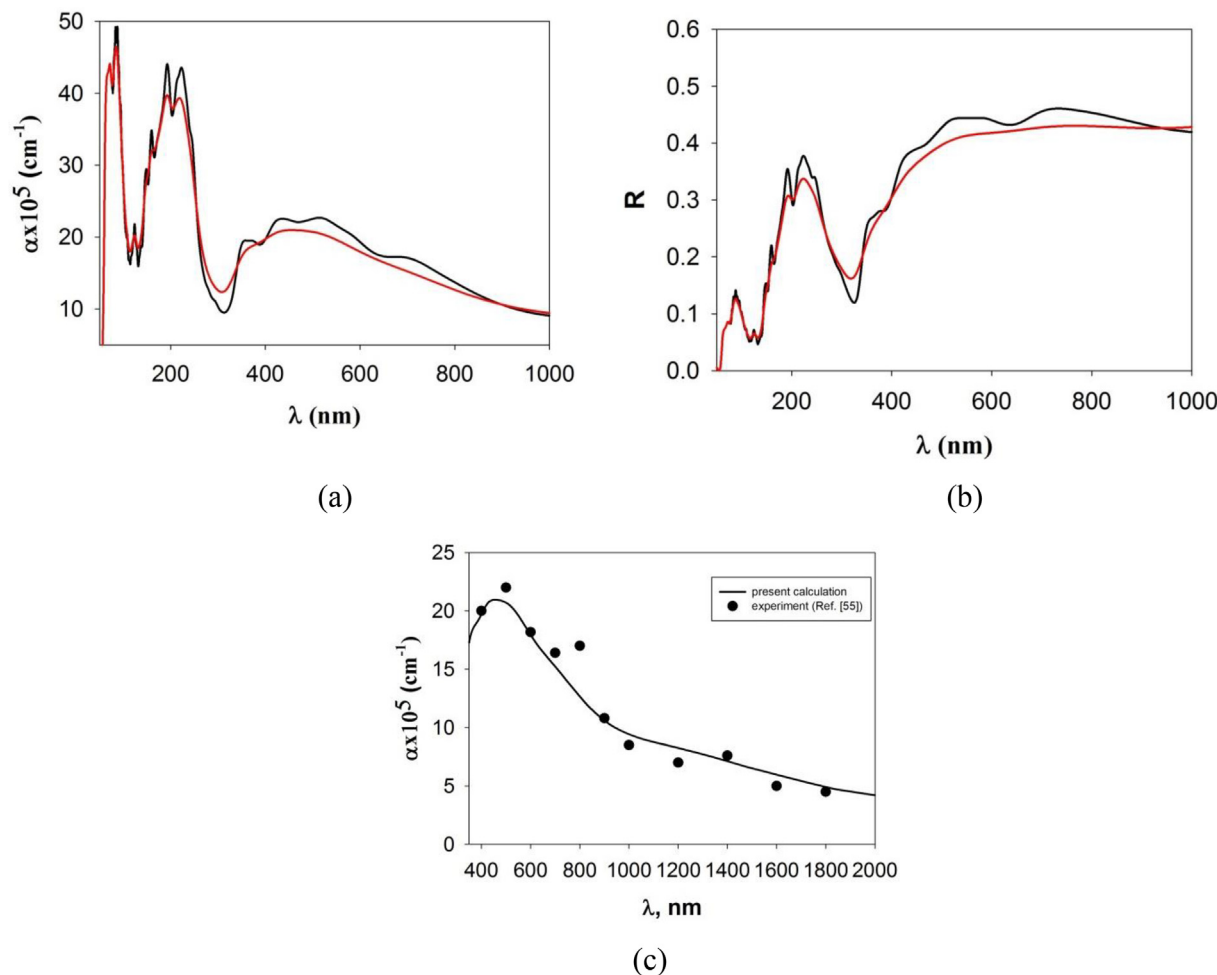
(a)

(b)

(c)

Fig. 4. Optical absorption (a) and reflection (b) spectra in GGA (black line) and G0W0 (red line) approximations; (c) the comparison of experimental and G0W0 absorption spectra. (For interpretation of the references to colour in this figure legend, the reader is referred to the web version of this article.)

behavior of spectral weights indeed shows that the d-electrons of Co ions have strong interaction.

In Fig. 4 we compare the dependencies of the optical properties of Co_3O_4, such as an absorption coefficient and a refractive index, on the wavelength within GGA and G0W0 approximations. As can be seen, both optical characteristics have a similar shape and behavior and the distinction between them are only slight. Absorption coefficients have two pronounced peaks in the UV region at wavelength about 50 and 200 nm. The analysis shows that the main contribution to the formation of the second peak comes from transitions from filled p-bands in the low-energy range to the empty d-bands (see Fig. 2b). In the range of low lambda the absorption peak arises due to the transitions from depth s-bands to the conductivity bands (not shown in Fig. 2). The energy of such transitions ($\omega \sim 20$–30 eV) just corresponds to the wavelengths $\lambda \sim 40 - 60$ nm. In the region of 350–800 nm, the broad absorption band is located. It is forming by the transitions from filled d-bands near the Fermi energy to empty d-bands. It should be mentioned that the behavior of the absorption spectrum in the range from 300 nm is close to experimentally obtained in Ref. [55] (Fig. 2c).

As known the crystal field leads to the split of d-electron states into threefold degenerated t2g- and twofold degenerated eg-states. Moreover, the tetrahedral symmetry tends to the decrease of eg-states energy and increase of energy of t2g-states, in the case of octahedral symmetry the situation is reversed. The contributions of t2g- and eg-states in the density of electronic states of both Co ions are shown in Fig. 5a and b and in Table 3 the occupation numbers of both Co ions are given. The Co^{3+} t2g-states are concentrated at the top of the valence

band, about -1 eV, while eg-states are centered at $+1.5$ eV. The Co^{2+} eg-states are located at about -0.5 eV and about -2.2 eV in the valence band, while t2g-states are hybridized with eg-states at -2.2 eV and give a contribution to the conduction band at $+0.8$ and 1.5 eV. As can be seen, Co^{3+} ion located in the octahedral environment has fully occupied low-lying minority and majority t2g-states while minority and majority overlying eg-states are almost empty. This results in the appearance of the low-spin state of Co^{3+} ion. As for Co^{2+} ion located in the tetrahedral environment, all low-lying eg-states and majority overlying t2g-states are filled by electrons, but minority overlying t2g-states are only partially filled. Thus, unpaired overlying t2g-electrons give a contribution to the appearance of the large magnetic moment on Co^{2+} ion.

3.2. Magnetic and optical properties under pressure

Since Co^{3+} ions are in a low-spin state the applied pressure can lead to the spin-crossover into the high-spin state of this ion. To check this possibility we performed the calculation of electronic and magnetic properties of Co_3O_4 under the tensile and compressive strain. The results are shown in Fig. 6 and Table 4. As seen from Fig. 6, the main peculiarity appears at the pressure P = -40 GPa. The magnetic moment on Co^{3+} ion has an abrupt leap from zero to almost 2 μB. Such a sharp appearance of the magnetic moment related to the redistribution of electrons between t2g and eg orbitals (Table 4). If at optimized parameter eg states were almost empty, at compressive pressure P = -40 GPa majority eg states shift below the Fermi energy, whereas minority
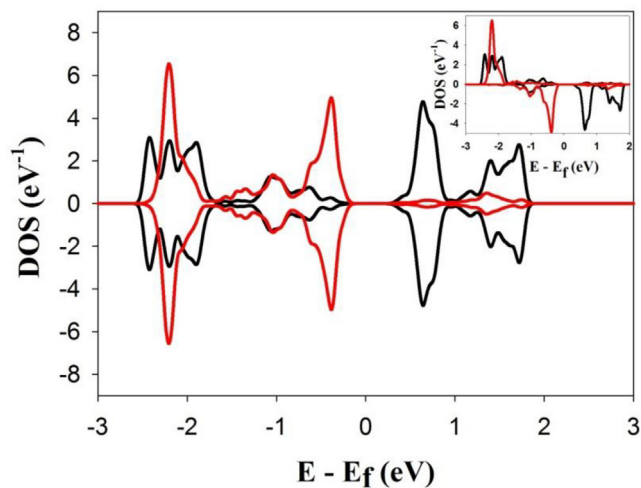
(a)
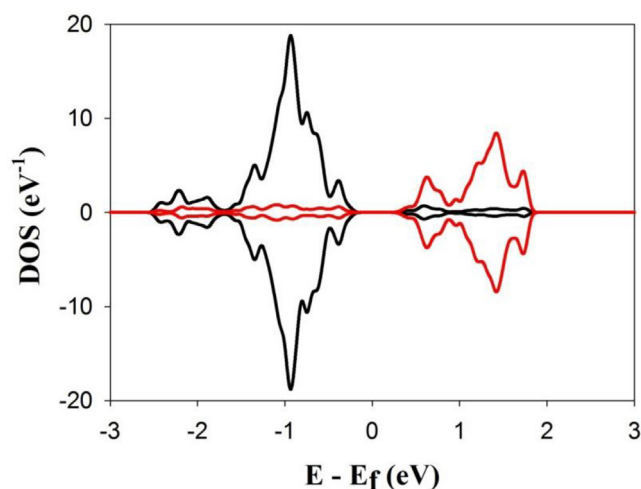
(b)

Fig. 5. Partial densities of d-electronic states (d-DOS) for Co^{2+} (a) and Co^{3+} (b) ions. Black lines show t2g-states, eg-states are shown by red line. The inset shows the d-DOS of one of two Co^{2+} ions. The zero on the energy axis is the Fermi energy. Negative values of DOS correspond to the spin-down states. (For interpretation of the references to colour in this figure legend, the reader is referred to the web version of this article.)

Table 3
Occupation numbers of Co ions in Co_3O_4.

d-state	Occupation numbers			
	Co^{2+}		Co^{3+}	
	major. state	minor. state	major. state	minor. state
t2g	1	0.27	1	1
eg	1	1	0.15	0.15

eg states stay almost empty. On the contrary, minority t2g states devastated by almost half, filling the majority eg-states (Fig. 7). So, we can suggest that electrons became more delocalized and smeared between orbitals resulting in an abrupt appearance of the magnetic moment. Such transition of Co^{3+} ion from low-spin state to the high-spin state opens a possibility for experimental control and change of the magnetic state of Co_3O_4 by pressure or strain. Notice that the similar behavior of Co^{3+} ion under was discussed in $GdCoO_3$ during expansion [56].
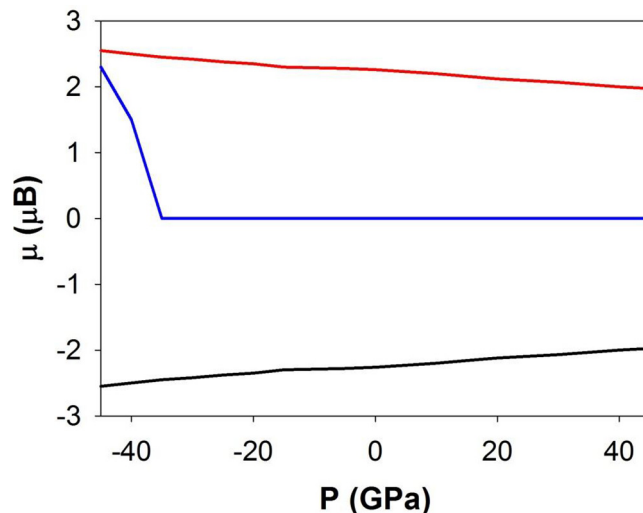

Fig. 6. The hydrostatic pressure dependencies of magnetic moments on Co^{3+} ion (blue line) and both Co^{2+} (red and black lines). (For interpretation of the references to colour in this figure legend, the reader is referred to the web version of this article.)

Table 4
Occupation numbers of Co^{2+} and Co^{3+} ions in the dependence on the hydrostatic pressure (P).

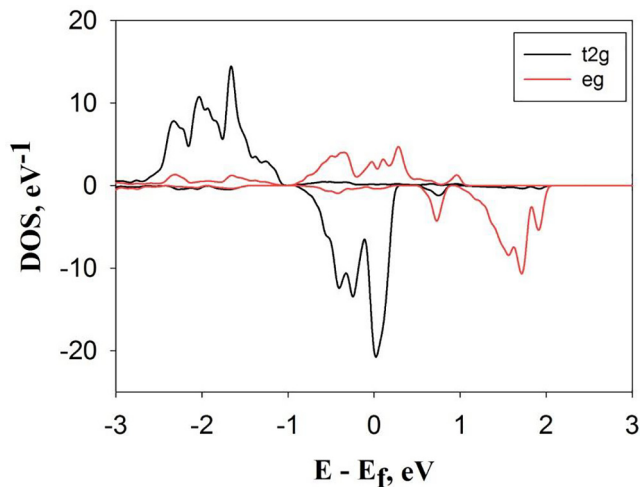| P (GPa)	d-state	Occupation numbers			
		Co^{2+}		Co^{3+}	
		major. state	minor. state	major. state	minor. state
0	t2g	1	0.27	1	1
	eg	1	1	0.15	0.15
−40	t2g	1	0.23	0.84	0.6
	eg	1	0.92	0.73	0.27

Fig. 7. Partial densities of d-electronic states (d-DOS) for Co^{3+} ion at the pressure P = −40 GPa. Black lines show t2g-states, eg-states are shown by red line. The zero on the energy axis is the Fermi energy. Negative values of DOS correspond to the spin-down states. (For interpretation of the references to colour in this figure legend, the reader is referred to the web version of this article.)

As for bandgap, it slightly decreases with positive hydrostatic pressure. The negative pressure, on the contrary, slightly increases the bandgap. However, at the critical pressure, when the spin-state
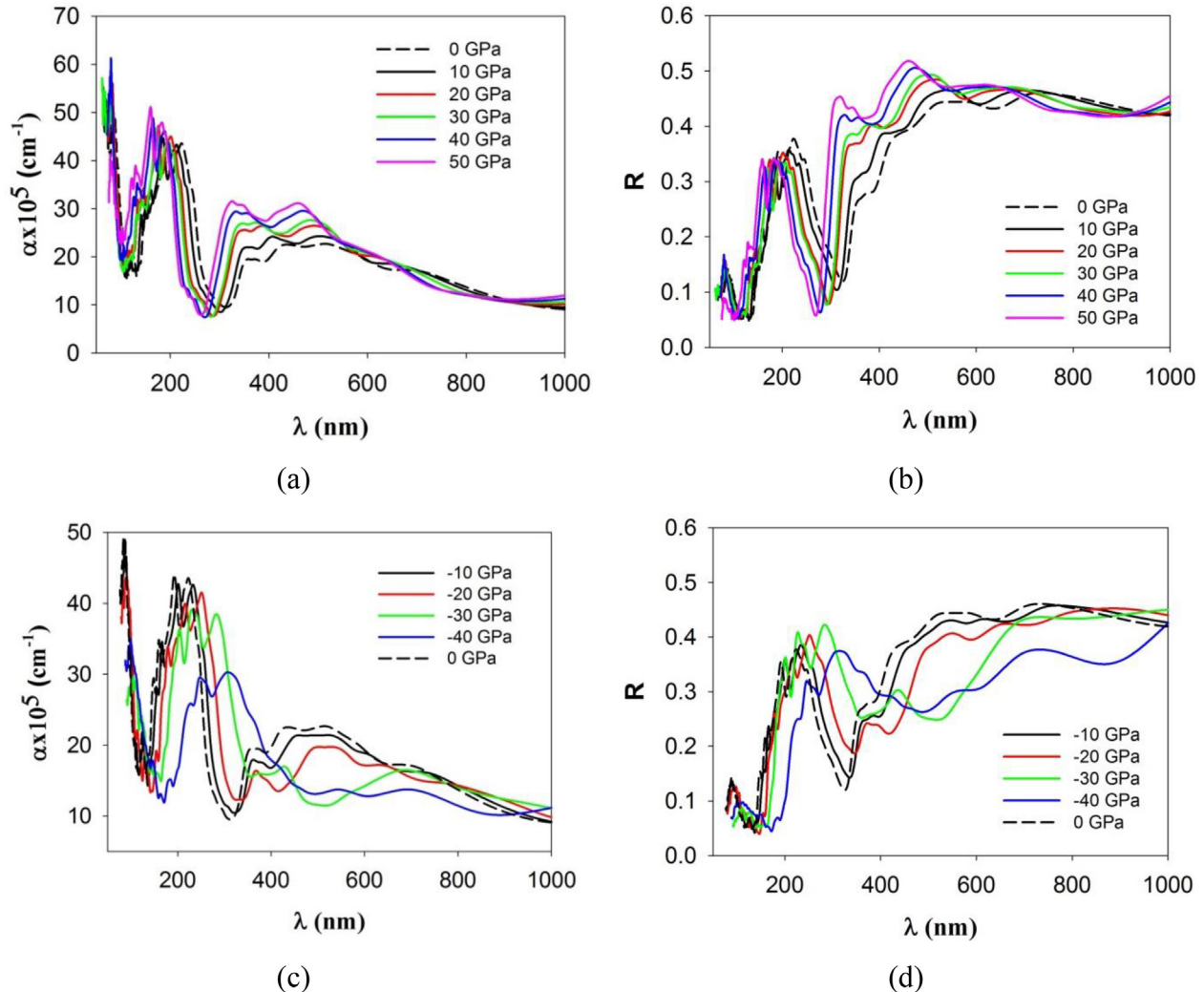
Fig. 8. Optical absorption (left) and reflection (right) spectra in the dependence on the positive (a, b) and negative (c, d) hydrostatic pressure.

transition occurs, the bandgap collapses due to the mentioned above redistribution of t2g- and eg-electrons, and the compound becomes metallic.

At last, in the Fig. 8 the dependencies of the absorption coefficient and refractive index under tensile and compressive hydrostatic pressure are shown. The compressive pressure shifts the absorption spectrum in the shortwave region and results in an increase of the absorption coefficient. The tensile pressure leads to the shift of the absorption spectrum in the longwave range and the absorption coefficient decrease. The same behavior is also observed for the refraction index.

4. Conclusion

In conclusion, we have performed the calculation of magnetic, electronic and optical properties of the antiferromagnetic insulating spinel Co_3O_4 within GGA, GGA + U, and G0W0 approximations. Since the GW approximations are more physically sound by construction due to the more accurate description of excited bands we believe that the obtained results would be useful for a deeper understanding of the physics of spinel with the transition metal. The calculation of Co_3O_4 within G0W0 approximations increases the bandgap comparing with GGA and GGA + U approximations. However, the agreement with the experiment is not as good as we expected. This can be related to the absence of self-consistency in G0W0 approximation what makes it sensitive to the input GGA band structure. The accounting for vertex corrections to GW also can help to improve the description of the gap.

Nevertheless, G0W0 approximation is the easiest way to calculate the energies of excitation bands and their spectral weights which are not available within the standard DFT approach. It was found that the GW calculations produced a decrease of the spectral weights of the quasi-particle bands down to 0.5. This indicates the presence of strong electronic d-d interactions. For a deeper understanding of the physics of these compounds and checking our predictions about the reduction in spectral weight, it would be useful to carry out ARPES (angle-resolved photoelectron spectroscopy) experiments on spinel Co_3O_4. The comparison of the optical spectra obtained in the ab initio calculations within the VASP in GGA and G0W0A shows that in general their shape and behavior are similar. Co_3O_4 has the large absorption peaks at about 50 nm and 200 nm and broad absorption band in the longwave range. The main contribution in the absorption in the visible light range is mainly given by d (Co)-d(Co) transitions, whereas peaks in the ultraviolet range came from p (O)-d (Co) transitions.

At last, we obtained that tensile pressure can lead to the abrupt appearance of the magnetic moment on Co^{3+} converting it from the low-spin state into the high-spin state due to the redistribution of d-electrons. This opens up the possibility of manipulating spin state by the strain that is important for the spintronics applications. So, our theoretical predictions can stimulate experimenters and technologists for designing new spintronics materials based on spinel Co_3O_4.

Declaration of Competing Interest

References

[1] V. Kocsis, S. Bordács, D. Varjas, K. Penc, A. Abouelsayed, C.A. Kuntscher, K. Ohgushi, Y. Tokura, I. Kézsmárki, Phys. Rev. B 87 (2013) 064416.
[2] V. Fritsch, J. Hemberger, N. Büttgen, E.-W. Scheidt, H.-A. Krug von Nidda, A. Loidl, V. Tsurkan, Phys. Rev. Lett. 92 (2004) 116401.
[3] R. Fichtl, V. Tsurkan, P. Lunkenheimer, J. Hemberger, V. Fritsch, H.-A. Krug von Nidda, E.-W. Scheidt, A. Loidl, Phys. Rev. Lett. 94 (2005) 027601.
[4] D. Santos-Carballal, A. Roldan, R. Grau-Crespo, N.H. de Leeuw, Phys. Rev. B 91 (2015) 195106.
[5] U. Lüders, A. Barthélémy, M. Bibes, K. Bouzehouane, S. Fusil, E. Jacquet, J.-P. Contour, J.-F. Bobo, J. Fontcuberta, A. Fert, Adv. Mater. 18 (2006) 1733.
[6] A. Krimmel, H. Mutka, M.M. Koza, V. Tsurkan, A. Loidl, Phys. Rev. B 79 (2009) 134406.
[7] J. García, G. Subias, J. Phys.: Condens. Matter 16 (2004) R145.
[8] M. Bibes, A. Barthelemy, IEEE Trans. Electron Devices. 54 (2007) 1003.
[9] M. Bibes, A. Barthelemy, Nature Mater 7 (2008) 425–426.
[10] J.M. Hu, Z. Li, L.Q. Chen, C.W. Nan, Nat. Commun. 2 (2011) 553.
[11] D.D. Awschalom, M.E. Flatt, Nat. Phys. 3 (2007) 153–159.
[12] Z.P. Xing, J.F. Li, D. Viehland, Appl. Phys. Lett. 91 (2007) 142905.
[13] H. Dery, P. Dalal, L. Cywmski, L.J. Sham, Nature 447 (2007) 573–576.
[14] Sagar E. Shirsath, M.H.N. Xiaoxi Liu, Adnan Younis Assadi, Yukiko Yasukawa, Sumanta Kumar Karan, Ji Zhang, Jeonghun Kim, Danyang Wang, Akimitsu Morisako, Yusuke Yamauchi, Sean Lia, Nanoscale Horizons 4 (2) (2019) 434–444.
[15] S.A. Wolf, D.D. Awschalom, R.A. Buhrman, J.M. Daughton, S. Von Molnar, M.L. Roukes, A.Y. Chtchelkanova, D.M. Treger, Science 294 (2001) 1488–1495.
[16] I. Zutic, J. Fabian, S.D. Sarma, Rev. Mod. Phys. 76 (2004) 323–386.
[17] S. Koshihara, A. Oiwa, M. Hirasawa, S. Katsumoto, Y. Iye, C. Urano, H. Takagi, H. Munekata, Phys Rev Lett 78 (1997) 4617–4620.
[18] H. Ohno, Nat. Mater. 9 (2010) 952–954.
[19] C. Bi, Y.H. Liu, T. Newhouse-Illige, M. Xu, M. Rosales, J.W. Freeland, O. Mryasov, S.F. Zhang, S.G.E.T. Velthuis, W.G. Wang, Phys. Rev. Lett. 113 (2014) 267202.
[20] Q.M. Zhang, Q. Li, R.L. Gao, W.P. Zhou, L.Y. Wang, Y.T. Yang, D.H. Wang, L.Y. Lu, Y.V. Du, Appl. Phys. Lett. 104 (2014) 142409.
[21] K. Sato, A. Matsuo, K. Kindo, Y. Kobayashi, K. Asai, J. Phys. Soc. Jpn. 78 (2009) 093702.
[22] S.W. Biernacki, Phys. Rev. B 74 (2006) 184420.
[23] H. Seo, A. Posadas, A.A. Demkov, Phys. Rev. B 86 (2012) 014430.
[24] X.W. Xie, Y. Li, Z.Q. Liu, M. Haruta, W.J. Shen, Nature 458 (2009) 746–749.
[25] M. Ando, T. Kobayashi, S. Iijima, M. Haruta, J. Mater. Chem. 7 (1997) 1779–1783.
[26] F. Svegl, B. Orel, M.G. Hutchins, K. Kalcher, J. Electrochem. Soc. 143 (1996) 1532–1539.
[27] W.Y. Li, L.N. Xu, J. Chen, Adv. Funct. Mater. 15 (2005) 851–857.
[28] F. Jiao, H. Frei, Angewandte Chemie International Edition 48 (2009) 1841–1844.
[29] L. Hu, Q. Peng, Y. Li, J. Am. Chem. Soc. 130 (2008) 16136–16137.
[30] W.L. Roth, J. Phys. Chem. Solids Pergamon Press. 25 (1964) l-10.
[31] L.M. Khriplovich, E.V. Kholopov, I.E. Paukov, J. Chem. Thermodyn. 14 (1982) 207–217.
[32] P. Dutta, M.S. Seehra, S. Thota, J. Kumar, J. Phys. Condens. Matter. 20 (2008) 015218.
[33] P.H.T. Ngamou, N. Bahlawane, Chem. Mater. 22 (2010) 4158–4165.
[34] K.J. Kim, Y.R. Park, Solid State Commun. 127 (2003) 25–28.
[35] L. Qiao, H.Y. Xiao, H.M. Meyer, J.N. Sun, C.M. Rouleau, A.A. Puretzky, D.B. Geohegan, I.N. Ivanov, M. Yoon, W.J. Weber, M.D. Biegalski, J. Mater. Chem. C. 1 (2013) 4628–4633.
[36] Y. Yamasaki, S. Miyasaka, Y. Kaneko, J.-P. He, T. Arima, Y. Tokura, Phys. Rev. Lett. 96 (2006) 207204.
[37] H. Murakawa, Y. Onose, S. Ohgushi, Y. Ishiwata, Y. Tokura, J. Phys. Soc. Jpn. 77 (2008).
[38] E. Kita, K. Siratori, K. Kohn, A. Tasaki, S. Kimura, I. Shindo, J. Phys. Soc. Jpn. 47 (1979) 1788.
[39] A.T.R. Dayalu, PhD thesys, Université Sciences et Technologies - Bordeaux I (2012).
[40] R. Saha, S. Ghara, E. Suard, D.H. Jang, K.H. Kim, N.V. Ter-Oganessian, A. Sundaresan, Phys. Rev. B 94 (2016) 014428.
[41] Xu. Xiang-Lan, Zhan-Hong Chen, Yi Li, Wen-Kai Chen, Jun-Qian Li, Surface Science 603 (2009) 653–658.
[42] Aron Walsh, Su-Huai Wei, Yanfa Yan, M.M. Al-Jassim, John A. Turner, Michael Woodhouse, B.A. Parkinson, Phys. Rev. B 76 (2007) 165119.
[43] Jia Chen, Wu Xifan, Annabella Selloni, Phys. Rev. B 83 (2011).
[44] S. Selcuk, A. Selloni, J. Phys. Chem. C 119 (18) (2015) 9973–9979.
[45] F. Aryasitiawan, O. Gunnarsson, Rep. Prog. Phys. 61 (1998) 237;
W.G. Aulbur, L. Jonsson, J.W. Wilkins, Solid State Phys. 54 (1999) 1.
[46] G. Kresse, J. Furthmüller, Phys. Rev. B 54 (1996) 11169.
[47] P.E. Blochl, Phys. Rev. B 50 (1994) 17953;
G. Kresse, D. Joubert, Phys. Rev. B. 59 (1999) 1758.
[48] J.P. Perdew, K. Burke, M. Ernzerhof, Phys. Rev. Lett. 77 (1996) 3865.
[49] H.J. Monkhorst, J.D. Pack, Phys. Rev. B 13 (1976) 5188.
[50] S.L. Dudarev, G.A. Botton, S.Y. Savrasov, C.J. Humphreys, A.P. Sutton, Phys. Rev. B 57 (1998) 1505.
[51] E. Sasıoglu, C. Friedrich, S. Blügel, Phys. Rev. B 83 (2011) 121101(R).
[52] M. Shishkin, G. Kresse, Phys. Rev. B 74 (2006);
F. Fuchs, J. Furthmuller, F. Bechstedt, M. Shishkin, G. Kresse, Phys. Rev. B 76 (2007).
[53] W.L. Smith, A.D. Hobson, Acta Crystallogr. B 29 (1975) 362.
[54] V.I. Anisimov, I.V. Solovyev, M.A. Korotin, M.T. Czyzyk, G.A. Sawatzky, Phys. Rev. B 48 (1993) 16929;
M.T. Czyzyk, G.A. Sawatzky, Rev. B 49 (1994) 14211;
A.I. Lichtenstein, M.I. Katsnelson, G. Kotliar, Phys. Rev. Lett. 87 (2001);
M.I. Katsnelson, A.I. Lichtenstein, Eur. Phys. J. B. 30 (2002) 9;
J. Kunes, V.I. Anisimov, A.V. Lukoyanov, D. Vollhardt, Phys. Rev. B 75 (2007);
B. Amadon, F. Lechermann, A. Georges, F. Jollet, T.O. Wehling, A.I. Lichtenstein, Phys. Rev. B 77 (2008);
(a) I. Leonov, A.I. Poteryaev, V.I. Anisimov, D. Vollhardt, Phys. Rev. Lett. 106 (2011);
M. Karolak, G. Ulm, T. Wehling, V. Mazurenko, A. Poteryaev, A. Lichtenstein, J. Electron Spectrosc. Relat. Phenom. 181 (2010) 11;
I.A. Nekrasov, N.S. Pavlov, M.V. Sadovskii, JETP Lett. 95 (2012) 581.
[55] S.A. Makhlouf, Z.H. Bakr, K.I. Aly, M.S. Moustaf, Superlattices and Microstructures 64 (2013) 107–117.
[56] Y.S. Orlov, L.A. Solovyov, V.A. Dudnikov, A.S. Fedorov, A.A. Kuzubov, N.V. Kazak, V.N. Voronov, S.N. Vereshchagin, N.N. Shishkina, N.S. Perov, K.V. Lamonova, R. Yu Babkin, Y.G. Pashkevich, A.G. Anshits, S.G. Ovchinnikov, Phys. Rev. B 88 (2013) 235105.